



**HAL**  
open science

# Tyrosine 105 and Threonine 212 at Outermost Substrate Binding Subsites -6 and +4 Control Substrate Specificity, Oligosaccharide Cleavage Patterns, and Multiple Binding Modes of Barley $\alpha$ -Amylase

Kristian Sass Bak-Jensen, Gwenaëlle André-Leroux, Tine E. Gottschalk, Gabriel Paës, Vinh Tran, Birte Svensson

## ► To cite this version:

Kristian Sass Bak-Jensen, Gwenaëlle André-Leroux, Tine E. Gottschalk, Gabriel Paës, Vinh Tran, et al.. Tyrosine 105 and Threonine 212 at Outermost Substrate Binding Subsites -6 and +4 Control Substrate Specificity, Oligosaccharide Cleavage Patterns, and Multiple Binding Modes of Barley  $\alpha$ -Amylase. *Journal of Biological Chemistry*, 2004, 279 (11), pp.10093-10102. 10.1074/jbc.M312825200 . hal-01607712

**HAL Id: hal-01607712**

**<https://hal.science/hal-01607712>**

Submitted on 31 May 2020

**HAL** is a multi-disciplinary open access archive for the deposit and dissemination of scientific research documents, whether they are published or not. The documents may come from teaching and research institutions in France or abroad, or from public or private research centers.

L'archive ouverte pluridisciplinaire **HAL**, est destinée au dépôt et à la diffusion de documents scientifiques de niveau recherche, publiés ou non, émanant des établissements d'enseignement et de recherche français ou étrangers, des laboratoires publics ou privés.

Copyright

# Tyrosine 105 and Threonine 212 at Outermost Substrate Binding Subsites –6 and +4 Control Substrate Specificity, Oligosaccharide Cleavage Patterns, and Multiple Binding Modes of Barley $\alpha$ -Amylase 1\*

Received for publication, November 24, 2003  
Published, JBC Papers in Press, December 1, 2003, DOI 10.1074/jbc.M312825200

Kristian Sass Bak-Jensen, Gwenaëlle André<sup>‡</sup>, Tine E. Gottschalk, Gabriel Paës<sup>‡§</sup>, Vinh Tran<sup>‡¶</sup>, and Birte Svensson<sup>||\*\*</sup>

From the Department of Chemistry, Carlsberg Laboratory, Gamle Carlsberg Vej 10, DK-2500 Copenhagen Valby, Denmark and the <sup>‡</sup>Laboratoire de Physico-Chimie des Macromolécules, INRA, BP 71627-44316 Nantes Cedex 03, France

The role in activity of outer regions in the substrate binding cleft in  $\alpha$ -amylases is illustrated by mutational analysis of Tyr<sup>105</sup> and Thr<sup>212</sup> localized at subsites –6 and +4 (substrate cleavage occurs between subsites –1 and +1) in barley  $\alpha$ -amylase 1 (AMY1). Tyr<sup>105</sup> is conserved in plant  $\alpha$ -amylases whereas Thr<sup>212</sup> varies in these and related enzymes. Compared with wild-type AMY1, the subsite –6 mutant Y105A has 140, 15, and <1% activity ( $k_{cat}/K_m$ ) on starch, amylose DP17, and 2-chloro-4-nitrophenyl  $\beta$ -D-maltoheptaoside, whereas T212Y at subsite +4 has 32, 370, and 90% activity, respectively. Thus engineering of aromatic stacking interactions at the ends of the 10-subsite long binding cleft affects activity very differently, dependent on the substrate. Y105A dominates in dual subsite –6/+4 [Y105A/T212(Y/W)]AMY1 mutants having almost retained and low activity on starch and oligosaccharides, respectively. Bond cleavage analysis of oligosaccharide degradation by wild-type and mutant AMY1 supports that Tyr<sup>105</sup> is critical for binding at subsite –6. Substrate binding is improved by T212(Y/W) introduced at subsite +4 and the [Y105A/T212(Y/W)]AMY1 double mutants synergistically enhanced productive binding of the substrate aglycone. The enzymatic properties of the series of AMY1 mutants suggest that longer substrates adopt several binding modes. This is in excellent agreement with computed distinct multiple docking solutions observed for maltododecaose at outer binding areas of AMY1 beyond subsites –3 and +3.

$\alpha$ -Amylases ( $\alpha$ -1,4-D-glucan glucanohydrolase, EC 3.2.1.1) hydrolyze internal  $\alpha$ -1,4-glycosidic bonds in starch and related dextrans and oligosaccharides (1). Substrate interactions along the extended binding site have traditionally been described by

\* This work was supported by the EU Biotech project (BIO4-CT98-0022) AGADE Alpha-Glucan Active Designer Enzymes) and a scholarship (to K. S. B.-J.) from Novo Nordisk A/S. The costs of publication of this article were defrayed in part by the payment of page charges. This article must therefore be hereby marked "advertisement" in accordance with 18 U.S.C. Section 1734 solely to indicate this fact.

<sup>‡</sup> Present address: U. M. R. FARE (INRA), 8 rue G. Voisin, 51686 Reims Cedex.

<sup>¶</sup> Present address: U.R. Biocatalyse (CNRS-FRE 2230), Faculté des Sciences et Techniques, 2 rue de la Houssinière, BP 92208, 44322 Nantes Cedex 3.

<sup>||</sup> Present address: Biochemistry and Nutrition Group, BioCentrum-DTU, Denmark Technical University, Søtafts Plads, Bldg. 224, DK-2800 Kgs. Lyngby, Denmark.

\*\* To whom correspondence should be addressed. Tel.: 45-3327-5345; Fax: 45-3327-4708; E-mail: bis@biocentrum.dtu.dk.

subsite maps that indicate the number of consecutive glucosyl binding subsites (ranging from 5–11), the cleavage position, and the affinity of substrate glucosyl residues at individual subsites (2–8). The binding cleft is formed by  $\beta \rightarrow \alpha$  loops of the catalytic ( $\beta/\alpha$ )<sub>3</sub> barrel domain (9–14). Due to enormous diversity in the binding loops, the  $\alpha$ -amylase family, also referred to as glycoside hydrolase clan H (GH-H)<sup>1</sup> consisting of glycoside hydrolase families 13 (GH13), 70, and 77 comprises almost 30 specificities (15–19). Substrate analogs are very rarely seen to fill the entire binding site in crystal structures, one example being a *Bacillus licheniformis*/*Bacillus amyloliquefaciens*  $\alpha$ -amylase chimera accommodating at subsites –7 through +3 a decasaccharide inhibitor derived by transglycosylation from the pseudotetrasaccharide acarbose (14). Related inhibitors cover the only five subsite long binding crevice in pancreatic  $\alpha$ -amylase (8, 9, 20), and occupy part of the longer binding sites in microbial  $\alpha$ -amylases (11, 13, 21) and in cyclodextrin glucosyltransferase (CGTase) (16, 22, 23). The structures validate modeled substrate complexes and subsite maps (8, 12, 24, 25) by highlighting (i) aromatic stacking and hydrogen bonds between carbohydrate and protein (9, 10, 21, 24, 26, 27), (ii) conformational features of the bound carbohydrate (8, 21, 28), (iii) conserved geometry of the catalytic site (10, 14, 15, 21, 22, 29, 30), and (iv) substrate binding motifs in  $\beta \rightarrow \alpha$  loops of the catalytic ( $\beta/\alpha$ )<sub>3</sub> barrel (15). The macromolecular substrate starch most probably also interacts with distinct areas outside the cleft as suggested by oligosaccharide occupation at so-called surface or secondary sites in several structures from GH-H (10, 14, 28, 31). This additional substrate binding is only proven, however, for starch binding domains of family 20 (afmb.cnr-mrs.fr/CAZY) found in ~10% of the GH13 members (32).

Barley  $\alpha$ -amylase 1 (AMY1) and AMY2 are among the most thoroughly described  $\alpha$ -amylases. The isozymes are synthesized in the seed aleurone layer during germination (33). They share 80% sequence identity and differ in activity, stability, and natural abundance (6) and they are speculated to play different roles in starch mobilization (34–38). The impact of

<sup>1</sup> The abbreviations used are: GH-H, glycoside hydrolase clan H; AMY1, barley  $\alpha$ -amylase isozyme 1; AMY2, barley  $\alpha$ -amylase isozyme 2; CGTase, cyclodextrin glucosyltransferase; Cl-PNPG<sub>7</sub>, 2-chloro-4-nitrophenyl  $\beta$ -D-maltoheptaoside; DP, degree of polymerization; ESI-MS, electrospray ionization mass spectrometry; GH10, glycoside hydrolase family 10; GH13, glycoside hydrolase family 13; GH70, glycoside hydrolase family 70; GH77, glycoside hydrolase family 77; PNPG<sub>5</sub>, 4-nitrophenyl  $\alpha$ -D-maltopentaoside; PNPG<sub>6</sub>, 4-nitrophenyl  $\alpha$ -D-maltohexaoside; PNPG<sub>7</sub>, 4-nitrophenyl  $\alpha$ -D-maltoheptaoside; S1, S2, and S3, docking solutions for AMY1/maltododecaose and AMY2/maltododecaose; MES, 4-morpholineethanesulfonic acid.

isozyme structural differences on activity has earlier been illustrated by mutations at subsites -5, -3, -2, -1, +1, and +2 in AMY1 (30, 39–43). The subsite map of both isozymes contains 10 consecutive subsites of varying affinity, *i.e.* subsites -6 through -1 from the catalytic site toward the non-reducing and subsites +1 through +4 toward the reducing end of the substrate (5). Consistent with this subsite organization barley  $\alpha$ -amylases release mainly oligosaccharides of DP 6–8 from starch (5–7), whereas most other  $\alpha$ -amylases give shorter products (1, 2, 44).

Few studies address GH-H substrate-subsite interactions far from the catalytic site (16, 39, 45). Subsite -6 in CGTase, however, was shown to control transglycosylation through induced fit at the catalytic site leading to formation of cyclodextrins by cyclization of the substrate glycone moiety (16, 45). The purpose of the present site-directed mutagenesis in AMY1 is to describe functional roles of the outermost subsites. A maltodex-rose complex was computed earlier by stepwise addition of glucosyl residues extending the acarbose molecule bound in AMY2 (10) beyond subsites -1 and +2. This complex revealed that Tyr<sup>104</sup><sub>AMY2</sub> and Tyr<sup>211</sup><sub>AMY2</sub> delimit the binding groove at subsites -6 and +4 (5, 25, 46, 47). The present incorporation and removal of aromatic residues at these positions in AMY1 thus manipulate common features in protein-carbohydrate interactions, *i.e.* stacking of aromatic side chains on carbohydrate rings and hydrogen bonding by the tyrosine  $\gamma$ OH or tryptophan  $\epsilon$ NH to carbohydrate OH groups (26, 27, 48, 49). The protein engineering strategy used took advantage of: (i) the modeled AMY2/maltodexrose (25), (ii) insight in earlier AMY1 mutants of substrate binding residues (4, 30, 39–41), and (iii) numerous crystal structures of  $\alpha$ -amylases from *Aspergillus oryzae* (21), *Aspergillus niger* (50), *B. licheniformis* (51), *Bacillus subtilis* (11), *Pseudoalteromonas haloplanktis* (29), AMY2 (10), porcine (9), and human pancreas (8), and other GH-H members; *e.g.* CGTase (16, 22, 52), TVAII  $\alpha$ -amylase (53), and amyloamylase (28). The enzymatic activities on starch, a short-chain amylose DP17, and various oligosaccharides of the eight mutants of AMY1 residues Tyr<sup>105</sup> and Thr<sup>212</sup> at subsites -6 and +4, including the AMY2 mimic [T212Y]AMY1, were interpreted using structural models established by AMY1/maltodexrose docking. Protein engineering at outer subsites turned out to have a great potential for manipulation of substrate and product specificities.

## EXPERIMENTAL PROCEDURES

### Strains and Plasmids

*Escherichia coli* DH5 $\alpha$  (Invitrogen) was used for standard cloning and *Pichia pastoris* GS115, pPIC3K, and pHIL-D2 (Invitrogen) for AMY1 expression; pHIL-D2 $\alpha$ 1 harboring AMY1 cDNA was an in-house stock (54). AMY1 cDNA clone E (38, 55) was a gift from John C. Rogers (Washington State University, Pullman).

### Plasmid Construction and Site-directed Mutagenesis

AMY1 cDNA is subcloned from pHIL-D2 $\alpha$ 1 at EcoRI sites into the pALTER-1 mutagenesis vector (Promega) to give pALTER- $\alpha$ 1. The EcoRI sites were used to subclone mutant AMY1 cDNA into p9000, a pPIC3K *P. pastoris* expression vector with bp 943–958 deleted upstream of the multiple cloning site to get AMY1 in-frame. p9000 $\alpha$ 1 containing wild-type AMY1 cDNA was constructed using the EcoRI sites. Three mutagenic primers (mutations in bold) 5'-TAGCCGCG-GCATCTTCTGCATCTTCGAGGGC-3' (Y105F), 5'-GGACAATATGGC-CCCCGGCGCGACGGCAAG-3' (T212P), and 5'-GGACAATATGGC-CTGGGGCGCGACGGCAAG-3' (T212W) were used (Altered Sites II System, Promega). Other mutants were made by megaprimer PCR (56) (DNA Engine Thermocycler, MJ Research). An upstream BamHI site (underlined) in the coding strand primer 5'-TTTGGATCCATGGGGAA-GAACGGC-3', and a downstream EcoRI site (underlined) in the template strand primer 5'-TTTGAATTCAGTGCAGACTTCAGCTCC-3' were used to subclone AMY1 cDNA into pPIC3K to get pPIC3K $\alpha$ 1. Mutant cDNA fragments were made using internal primers 5'-TAGC-

CGCGCATCGCCTGCATCTTCGAGGGC-3' (Y105A), 5'-TAGCCGCG-GCATCTGGTGCATCTTCGAGGGC-3' (Y105W), and 5'-GGACAATAT-GGCCTACGGCGCGACGGCAAG-3' (T212Y). Double mutants were constructed by subcloning a DNA fragment encoding Y105A into the T212(Y/W) expression vectors. Standard recombinant DNA techniques were used (57), and sequences were confirmed by chain terminator sequencing (58) using a 377-DNA Sequenator or ABI PRISM 310 Genetic analyzer (PerkinElmer Life Sciences).

### Transformation and Screening of *P. Pastoris*

Mutated pPIC3K $\alpha$ 1 or p9000 $\alpha$ 1 (~40  $\mu$ g) was linearized by BglII (Promega) prior to electroporation of *P. pastoris* followed by plate screening on MD (minimal dextrose; 1.34% YNB, 2% glucose, 0.4  $\mu$ g  $\times$  ml<sup>-1</sup> D-biotin, 1.5% agar) for His<sup>+</sup> phenotype, MM (as MD, but with 0.5% glucose replacing methanol) for Mut<sup>s</sup> (methanol slow utilization) phenotype, indicating integration of the expression cassette into the AOX1 locus, and MM, 2% soluble potato starch, to detect secretion of active  $\alpha$ -amylase (39).

### Recombinant AMY1 Production and Purification

Transformants were grown (600 ml of BMGY: 0.1 M potassium phosphate, pH 6.0, 0.67% YNB, 0.4  $\mu$ g  $\times$  ml<sup>-1</sup> D-biotin, 1% glycerol, 1% yeast extract, 2% peptone) in 5-liter flasks with shaking (30 °C, 225 rpm, 2 days) to OD<sub>600</sub>  $\approx$  20. Cells were harvested (20 °C, 1500 rpm, 8 min, Beckman J6-MC centrifuge), resuspended for induction (300 ml of BMMY, as BMGY but with 0.5% methanol replacing glycerol), and grown (24 h).  $\alpha$ -Amylase activity (Phadebas test; Amersham Biosciences) and AMY1 amounts (estimated from silver-stained SDS-PAGE using purified AMY1 as standard) were monitored in supernatants (54). *P. pastoris* secreted 6–85 mg  $\times$  liter<sup>-1</sup> AMY1 mutants and wild type. Cell harvest and induction were repeated up to three times. The combined supernatants were added 5% (w/v) (NH<sub>4</sub>)<sub>2</sub>SO<sub>4</sub>, 0.02% NaN<sub>3</sub>, applied to  $\beta$ -cyclodextrin-Sepharose (diameter 2.6 cm; 20 mM sodium acetate, pH 5.5, 25 mM CaCl<sub>2</sub>; 1 ml resin per mg AMY1) (37), washed by buffer (0.2 M in NaCl; 20 column volumes), and eluted by 8 mg  $\times$  ml<sup>-1</sup>  $\beta$ -cyclodextrin (2 column volumes). Fractions with activity were pooled, concentrated to 2 mg  $\times$  ml<sup>-1</sup> (Centriprep, 10 kDa cut-off, Millipore), dialyzed (10 mM MES, pH 6.7, 25 mM CaCl<sub>2</sub>), added 0.02% NaN<sub>3</sub>, and stored at 4 °C.

### Protein Characterization

SDS-PAGE (10–15%) and IEF (pH 4–6.5) (Phast-System, Amersham Biosciences) of 0.2–0.5  $\mu$ g of protein were silver stained (39) or immunoblotted using rabbit anti-AMY2 immune serum (37). IEF gels were soaked in 2% soluble potato starch and zymograms developed as described (37). AMY1 mutants and wild type migrated as single bands of  $M_r$   $\sim$  45,000 (SDS-PAGE) but gave three major bands of pI 4.7–5.1 in IEF. This pattern always recurs for recombinant AMY1 due to inactivating glutathionylation of C95 and C-terminal trimming (39, 54, 55). Individual forms of [Y105A/T212W]AMY1 were resolved by anion exchange chromatography (ResourceQ, 6 ml; Amersham Biosciences) as described (39), dialyzed (1 nmol) against water (4 °C, Slide-A-Lyzer cassettes, 10-kDa cut-off, Pierce) and subjected to ESI-MS (39) (55) and N-terminal sequencing (0.2 nmol) (Applied Biosystems Model 470A Sequenator; Model 120A PTH-Analyzer). This confirmed partial C95-glutathionylation, C-terminal trimming, and correct N-terminal processing and suggested di- and trimannosylation of Thr<sup>410</sup> (39, 54, 55, 59, 60). Since mutants and wild-type AMY1 showed essentially the same distribution of forms in IEF, the enzymatic properties were characterized without prior removal of the C95-glutathionylated form that constituted  $\sim$ 10%. Protein concentrations were calculated from amino acid contents (Amersham Biosciences/LKB Alpha Plus amino acid analyzer) in hydrolysates (6 M HCl, 110 °C, 24 h) of 15–40  $\mu$ g of protein.

### Assays and Enzyme Kinetics

**Insoluble Blue Starch**—Blue starch (customer preparation, Amersham Biosciences) at 10 concentrations (0.1–12.5 mg  $\times$  ml<sup>-1</sup>; 20 mM sodium acetate, pH 5.5, 5 mM CaCl<sub>2</sub>, 0.005% bovine serum albumin; 4 ml) was added enzyme (0.8–1.2 units) at 37 °C. The reaction was stopped after 15 min (0.5 M NaOH; 1 ml) followed by centrifugation (16,000  $\times$  g, 2 min) and OD<sub>620</sub> measurement of supernatants (300  $\mu$ l; microtiter plate reader; Ceres UV-900-HDi scanning autoreader, Bio-Tek Instrument). One activity unit is the amount of enzyme that during 15 min gives  $\Delta$ OD<sub>620</sub> = 1 in the final volume.  $k_{cat}$  and  $K_m$  were obtained by fitting hydrolysis rates to the Michaelis-Menten equation (GraFit 3.01; Erithacus Software Ltd.). The routine assay has 6.25 mg  $\times$  ml<sup>-1</sup> substrate (54).

**Amylose**—Initial rates of hydrolysis of amylose DP17 (average degree of polymerization of 17; Hayashibara, Okayama, Japan) at 8 concentrations (0.04–10.8 mg  $\times$  ml<sup>-1</sup>) were determined in the above buffer by adding enzyme (2–4 nM) at 37 °C (35) and measuring reducing sugar by the copper-bicinchoninate procedure (61).  $A_{540}$  was measured using maltose (2.5–20  $\mu$ g  $\times$  ml<sup>-1</sup>) as standard, and  $k_{\text{cat}}$  and  $K_m$  were calculated as above.

**2-Chloro-4-nitrophenyl  $\beta$ -D-Maltoheptaoside (Cl-PNPG<sub>7</sub>)**—Initial hydrolysis rates at 8 concentrations (0.15–13.8 mM) of Cl-PNPG<sub>7</sub> were measured at  $A_{405}$  in triplicate (wild-type: 1–4 nM; mutants: 1–40 nM) at 30 °C using Granustest 3 kit (Merck; phosphate buffer pH 6.8, 0.005% bovine serum albumin; total volume, 100  $\mu$ l) (35) using 2-chloro-4-nitrophenol (Merck) as standard and used to calculating  $k_{\text{cat}}$  and  $K_m$  as above.

#### Oligosaccharide Bond Cleavage

1 mM 4-nitrophenyl  $\alpha$ -D-maltopentaoside, -hexaoside, or -heptaoside (PNPG<sub>5</sub>, PNPG<sub>6</sub>, Fluka; PNPG<sub>7</sub>, Roche Applied Science) was hydrolyzed by 333, 66.7, and 6.7 nM enzyme (20 mM sodium acetate, pH 5.5, 5 mM CaCl<sub>2</sub>; 60  $\mu$ l) for 15 s to 35 min at 37 °C. The reaction was stopped (1.75 M acetic acid; 10  $\mu$ l) at 10 or 35% substrate conversion. Samples (10  $\mu$ l) were automatically injected (WISP 710A, Waters) via a 5- $\mu$ l Hypersil APS2 Guard column onto a 250 mm  $\times$  4 mm 5  $\mu$ l Hypersil APS2 column, eluted (70% CH<sub>3</sub>CN aq.; 0.70 ml  $\times$  min<sup>-1</sup>; Waters 510 pumps) at 30 °C (Supertherm Incubator, MicroLab, Denmark). Mixtures of PNP (Sigma), PNPG<sub>1-7</sub> (PNPG<sub>1</sub> and PNPG<sub>2</sub>, Sigma; PNPG<sub>3</sub>, Roche Applied Science; PNPG<sub>4</sub>, Calbiochem) in 20 mM sodium acetate, 0.25 M acetic acid, pH 4, 5 mM CaCl<sub>2</sub> (retention: 4–18 min) enabled quantification at 313 nm (SPD-6A UV Spectrophotometric Detector, Shimadzu). Standards, substrate, and controls with buffer replacing enzyme or substrate were run between samples. The cleavage frequency for individual substrate bond was calculated from averages of formed products in triplicate analyses (S.D.  $\leq$ 2%).

#### Molecular Modeling of AMY2 and AMY1/Maltododecaose

As the AMY1 structure was not available, AMY1/maltododecaose was built by homology modeling using as template AMY2/maltododecaose extended from AMY2/maltododecaose (10, 25, 46, 47) (PDB 1BG9, Ref. 62). Use of maltododecaose avoided edge effects on binding energies computed for subsites -6 and +4. To save CPU time AMY2 was truncated to  $(\beta/\alpha)_8$  barrel segments forming the binding site; Gln<sup>5</sup>-His<sup>14</sup> ( $\beta_1 \rightarrow \alpha_1$ ), Ser<sup>43</sup>-Leu<sup>56</sup> ( $\beta_2 \rightarrow \alpha_2$ ), Asp<sup>87</sup>-Asp<sup>148</sup> ( $\beta_3 \rightarrow \alpha_3$ ), Phe<sup>178</sup>-Ser<sup>185</sup> ( $\beta_4 \rightarrow \alpha_4$ ), Ala<sup>203</sup>-Leu<sup>228</sup> ( $\beta_5 \rightarrow \alpha_5$ ), Thr<sup>243</sup>-Val<sup>256</sup> ( $\beta_6 \rightarrow \alpha_6$ ), Thr<sup>283</sup>-Pro<sup>300</sup> ( $\beta_7 \rightarrow \alpha_7$ ). The backbone was fixed at segment ends having no substrate contact to maintain structural integrity during energy minimization. AMY1/maltododecaose was calculated after introducing 33 AMY1 residues in AMY2/maltododecaose and checking side-chain orientation. AMY1 mutants were simulated using the same procedure. For each docking solution energy minimization steps (20,000 iterations each) were done with visual inspection of structural consistency and manual reorientation of side chains and maltododecaose OH groups if needed. The same maximum derivative criterion was used for minimization steps and to stop refinement. Although highly refined docking solutions resulted from 5–9 steps and local rearrangement, all local minima were not necessarily explored.

#### Subsite Binding Energy Computation

Comparison of docking solutions used relative energies, and electrostatic and van der Waals non-bonded energy terms between enzyme and substrate were assumed to represent the total interaction energy. The contribution of each subsite was estimated for bound glucose and amino acid residues with at least one heavy atom  $\leq$ 4.0 Å from a glucose heavy atom. By further isolation of subsets of atoms, hydrogen bonding and stacking terms were discriminated and a van der Waals interaction term was defined by subtraction from the total energy. This segregation of subsites only considered short and medium distance energy terms, hence the sum of subsite binding energies differed slightly from the total docking energy.

## RESULTS

**Design and Production of Mutants at Outermost Subsites**—Positions to be replaced were identified in AMY2/maltododecaose as Tyr<sup>104</sup><sub>AMY2</sub>, which stacked onto substrate at subsite -6, and Tyr<sup>211</sup><sub>AMY2</sub>  $\gamma$ OH of which formed a hydrogen bond with glucose O6 at subsite +3 (25). Mutants were made in AMY1 because of the absence of an efficient heterologous AMY2 expression sys-

tem. Plant  $\alpha$ -amylases invariantly contain the Tyr<sup>105</sup><sub>AMY1</sub> (Tyr<sup>104</sup><sub>AMY2</sub>) (Fig. 1). Since Tyr<sup>105</sup><sub>AMY1</sub> is situated in the variable domain B (15) equivalent residues were not recognized in other  $\alpha$ -amylases. Thr<sup>212</sup><sub>AMY1</sub> (Tyr<sup>211</sup><sub>AMY2</sub>) on the other hand belongs to the  $\beta \rightarrow \alpha 5$  sequence motif of the  $(\beta/\alpha)_8$  barrel domain that includes two more substrate binding residues Trp<sup>207</sup><sub>AMY1</sub> and Asn<sup>209</sup><sub>AMY1</sub> and the catalytic acid/base Glu<sup>205</sup><sub>AMY1</sub> (10, 42). Most plant  $\alpha$ -amylases have Tyr, as Tyr<sup>211</sup><sub>AMY2</sub>, but Thr as Thr<sup>212</sup><sub>AMY1</sub>; Asn, Gln, and Gly also occur. This motif easily aligns with other GH-H clan members (10, 15, 63, 64) having Ala, Asp, Glu, Met, and Pro (Fig. 1). Thus to manipulate aromatic substrate stacking, Tyr<sup>105</sup><sub>AMY1</sub> was replaced by Ala, Phe, and Trp, and Thr<sup>212</sup><sub>AMY1</sub> by Pro, Tyr, and Trp. Y105A and T212(Y/W) were furthermore combined to swap the aromatic group from an outer glycone to an outer aglycone binding subsite. The replacements were compatible with the structure, AMY1/maltododecaose modeling suggesting that Y105(F/W) stack onto substrate at subsite -6 and that T212(Y/W) mimic Tyr<sup>211</sup><sub>AMY2</sub> substrate interactions at subsites +3 and +4 (not shown).

**Enzymatic Properties of Mutants at Subsite -6**—Immense variation in effect of Y105A mutation on activity for various substrates (Table I) suggested the presence of more than one binding mode. Both affinity and turnover of Cl-PNPG<sub>7</sub> by Y105A AMY1 were very low, while for amylose DP17  $k_{\text{cat}}$  was essentially unchanged and  $K_m$  increased 4-fold compared with wild type, a trend becoming more prominent for insoluble Blue Starch showing increased  $k_{\text{cat}}$  and unchanged  $K_m$  (Table I). In contrast, the conservative Y105(F/W) mutants resembled wild-type AMY1 closely, Y105F and Y105W being slightly superior on starch and on both Cl-PNPG<sub>7</sub> and amylose DP17, respectively. The loss of the substrate binding  $\gamma$ OH group in Y105F decreased affinity (3-fold) only for Cl-PNPG<sub>7</sub> (Table I).

**Enzymatic Properties of Mutants at Subsite +4**—The three T212(P/Y/W) caused changes very different from the Tyr<sup>105</sup> mutants. [T212(Y/W)]AMY1 were particularly favorable on amylose DP17 (Table I), increasing the affinity 5- and 2-fold and  $k_{\text{cat}}/K_m$  to 370% of T212Y and 180% of T212W compared with wild type. While affinity of T212W also improved substantially for both Cl-PNPG<sub>7</sub> and starch, T212Y, the AMY2 mimic, surprisingly lost affinity for both substrates. T212P diverged and underwent the largest decrease in affinity, but retained  $k_{\text{cat}}$  for starch in contrast to [T212(Y/W)]AMY1, and had the highest  $k_{\text{cat}}$  and  $k_{\text{cat}}/K_m$  for amylose DP17 and Cl-PNPG<sub>7</sub>, respectively (Table I).

**Effects of Dual Mutation at Subsites -6 and +4**—Simultaneous changes were imposed upon both ends of the binding cleft in [Y105A/T212(Y/W)]AMY1. For amylose DP17, these double mutants displayed the full loss in affinity of [Y105A]AMY1 and had the lowest  $k_{\text{cat}}$  of all mutants, while kinetic parameters on Cl-PNPG<sub>7</sub> and starch mostly were intermediate to the values of the corresponding single mutants (Table I). The much reduced transition state stabilization ( $k_{\text{cat}}/K_m$ ) for amylose DP17, for which remarkably the important decrease in  $K_m$  of the single T212(Y/W) mutants seemed without effect, disclosed a critical interdependence of the outermost subsites acting on the maltodextrin. In contrast, introduction of T212(Y/W) greatly ameliorated the poor activity of Y105A on Cl-PNPG<sub>7</sub> and [Y105A/T212(Y/W)]AMY1 also on starch kept the trend of the single T212W being more active than [T212Y]AMY1 (Table I). Noticeably,  $K_m = 1.0\%$  for starch of Y105A/T212Y was higher than of both the corresponding single mutants and AMY2 ( $K_m = 0.5\%$ ) (65), which T212Y is mimicking.

**Relative Specificity**—A major general goal when developing of  $\alpha$ -amylases and related enzymes is modification of specificity

Enzyme	Sequence		Sequence		Source	Accession
	Y105 ↓		$\beta$ 5 * EEEE	T212 ↓		
$\alpha$ -Amylase	99	KDSRGIYCIFEGG	201	LVAEVVDNMATGG	Barley (AMY1)	Plant P00693
	98	..G.....	200	F...I.TSL.Y..	Barley (AMY2)	P04063
	99	.....	202	....L..S..Y..	Rice (2A)	P27935
	99	.....	201	.....T.P...	Oat	CAA09324
	98	..G....V....	200	FV...I.SSLHYD.	Maize	Q41770
	98	..G..V.....	200	FV.G.LY.RDRQLL	Wheat (AMY3)	P08117
	97	..G.....	199	F..G.K..SISY.Q	Mung bean	P17859
	97	..G.....	199	F..G.K..PLSYEN	Kidney bean	BAA33879
	99	.....L....	201	F..G.F.NSL.Y.S	Dodder	AAA16513
	96	QGHG.M.NRYD.I	190	F..G.Y..TCNYK.	Potato	M79328
			229	FIFQ..I.LGGEAI	Hog	Mammal P00690
			226	YCIQ..L.GDPAYT	<i>A. oryzae</i>	Fungus P10529
			227	YS.G..FQGDPAIT	<i>S. fibuligera</i>	Yeast P21567
			257	FT...Y.Q.DLGAL	<i>B. licheniformis</i>	Bacterium P06278
			257	FT...Y.Q.N.GKL	<i>B. amyloliquefaciens</i>	P00692
			353	YILG.I.HDSLPLW	<i>B. acidopullulyticus</i>	P32818
			926	FTMG.IFHGDPAIV	<i>P. polymyxa</i>	P21543
		261	FI...Y.SHEVDKL	<i>E. coli</i>	P26612	
		249	FL.G.WYGDDEGTA	<i>B. stearothermophilus</i>	P19531	
G4-forming amylase		215	FC.G.L.KGPSEYYP	<i>P. saccharophila</i>	P22963	
Neopullulanase		353	YILG.I.HDAMPWL	<i>B. stearothermophilus</i>	P38940	
Cyclodextrinase		350	II.G...HDASPWL	<i>T. ethanolicus</i>	P29964	
Oligo-1,6-glucosidase		251	MT.G.MPGVTTEEA	<i>B. cereus</i>	P21332	
Pullulanase		390	YI.G.I..YRPEWL	<i>D. mucosus</i>	Q9HHB0	
Isoamylase		431	DLF..P.AIGGNSY	<i>P. amyloclavata</i>	P10342	
Cyclomaltodextrin glucanotransferase		253	FTFG.WFLGS.ASD	<i>B. circulans</i>	P30920	
Sucrose phosphorylase		230	EILP.IHEHYSIPK	<i>L. mesenteroides</i>	Q59495	
Amylosucrase		332	FFKS.AIVHPDQVV	<i>N. polysacchara</i>	Q92E02	
4-glucanotransferase		212	IFL..I.AEARMDV	<i>T. maritima</i>	Q60035	
Amylomaltase		336	PVL..DLGVITPEV	<i>T. aquaticus</i>	O87172	
Dextranase		449	VSIV.A.SDND.PY	<i>S. downei</i>	AAC63063	
Starch branching enzyme IIa		433	VSIG.DVSG.P.FC	Barley	Plant AF064560	
$\alpha$ -Glucosidase (MAL3S)		272	MT.G..AHGSDNAL	<i>S. cerevisiae</i>	Yeast P38158	

FIG. 1. Alignment of amino acid sequences for  $\alpha$ -amylases and related enzymes near Tyr<sup>105</sup> and Thr<sup>212</sup> in AMY1. Only plant  $\alpha$ -amylase sequences are aligned for Tyr<sup>105</sup>. For Thr<sup>212</sup> non-plant  $\alpha$ -amylases and other GH-H members are included. Residues in AMY2  $\beta$ -strand 5 (17) are indicated ( $\beta$ 5) as is Glu<sup>205</sup> (E205, \*), the catalytic acid/base. Identity to AMY1 is indicated by a dot.

TABLE I  
Enzymatic properties of AMY1 subsite -6 and +4 mutants towards Cl-PNPG<sub>7</sub>, amylose DP17, and insoluble Blue Starch

Enzyme	Cl-PNPG <sub>7</sub>			Amylose DP17			Blue Starch			Specificity ratios	
	$k_{cat}$	$K_m$	$k_{cat}/K_m$	$k_{cat}$	$K_m$	$k_{cat}/K_m$	$k_{cat}^a$	$K_m$	$k_{cat}/K_m$	BS:Cl-PNPG <sub>7</sub>	BS:DP17
	$s^{-1}$	mM	$s^{-1} \times mM^{-1}$	$s^{-1}$	$mg \times ml^{-1}$	$s^{-1} \times mg^{-1} \times ml$	$units \times mg^{-1}$	$mg \times ml^{-1}$	$units \times mg^{-1} \times ml$	$(k_{cat}/K_m)_{Cl-PNPG_7}$	$(k_{cat}/K_m)_{DP17}$
Wild type	119 ± 6.5	1.7 ± 0.13	70	165 ± 8	0.57 ± 0.09	289	2900	0.4	7250	103	25
Y105A/T212Y	31 ± 1.2	6.0 ± 0.44	5	78 ± 5	2.27 ± 0.14	34	2100	1.0	2100	425	61
Y105A/T212W	24 ± 0.6	3.1 ± 0.29	8	105 ± 15	2.00 ± 0.09	53	2900	0.3	9667	1210	182
Y105A	(<10)	(>10)		146 ± 15	2.36 ± 0.66	62	4000	0.4	10000		161
Y105F	203 ± 12	4.9 ± 0.70	41	158 ± 5	0.58 ± 0.06	272	3200	0.4	8000	195	29
Y105W	132 ± 2.2	1.3 ± 0.08	102	200 ± 6	0.48 ± 0.13	417	2600	0.5	5200	71	17
T212P	140 ± 4.3	1.4 ± 0.15	100	264 ± 21	0.48 ± 0.13	550	3000	1.5	2000	20	3.6
T212Y	127 ± 6.4	2.0 ± 0.28	64	127 ± 4	0.12 ± 0.02	1079	1500	0.6	2500	39	2.3
T212W	61 ± 1.4	0.6 ± 0.07	102	154 ± 6	0.29 ± 0.03	531	1700	0.3	5667	56	10.7

<sup>a</sup> Kinetic parameters were obtained as described under "Experimental Procedures."

without loss of the wild-type activity level. This was successfully achieved for Y105A/T212W and Y105A both very clearly preferring starch, and T212Y favoring amylose, while [T212(P/W)]AMY1 acted favorably on both oligosaccharide and amylose, in all cases with higher activity than wild type (Table I). The important variation in  $k_{cat}/K_m$  ratios for insoluble Blue Starch: Cl-PNPG<sub>7</sub> and insoluble Blue Starch: amylose DP17 by factors of 0.2–12 and 0.1–7 of the wild-type ratios, respectively, encourages further development of relative substrate specificity through rational protein engineering.

**Effects of Mutations on Oligosaccharide Action Patterns**—Mutation at specific subsites can reposition short substrates in the binding cleft resulting in product profile engineering (39–41, 66). Most unusually Y105A and [Y105A/T212(Y/W)]AMY1 produced substantial amounts of PNPG<sub>2</sub> and PNPG<sub>3</sub> from PNPG<sub>7</sub> and less PNPG, which is the predominant wild-type

product, thus reflecting relative gain and loss of aglycone and glycone binding, respectively (Fig. 2). Noticeable both T212(Y/W), like other single subsite mutants (30, 39–41), were unable to pull PNPG<sub>7</sub> off subsite -6 (Fig. 2). PNPG<sub>6</sub> got more or less displaced in the mutants, except T212P. Thus [T212(Y/W)]AMY1 counterbalanced the wild-type subsite -6 Tyr<sup>105</sup> contact, and both double mutants reinforced the effect of Y105A to release only traces of PNP, the major product of AMY1 wild type (Fig. 2). Modest sliding of PNPG<sub>6</sub> toward the aglycone binding area also in [Y105(F/W)]AMY1 indicated that these aromatic substitutions weakened subsite -6 interactions, consistent with Tyr<sup>105</sup> in wild type being invariant in plant  $\alpha$ -amylases (Fig. 1). Finally, PNPG<sub>5</sub> cannot cover subsite -6 in productive complexes, and the action pattern was insensitive to Tyr<sup>105</sup> mutations, while aromatic side chains introduced at subsite +4 promoted aglycone binding (Fig. 2). Transglycosy-

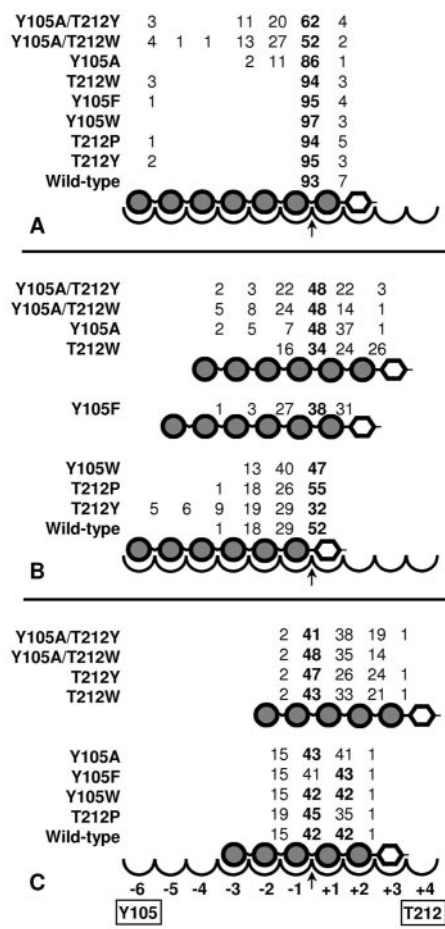


FIG. 2. Oligosaccharide action patterns of AMY1 wild type and mutants. Bond cleavage frequencies were determined for AMY1 wild type and mutants acting on PNPNG<sub>7</sub> (A), PNPNG<sub>6</sub> (B), and PNPNG<sub>5</sub> (C) (see “Experimental Procedures”). In wild-type AMY1 outer subsites -6 and +4 contain Tyr<sup>105</sup> and Thr<sup>212</sup>, respectively. The catalytic site, situated between subsites -1 and +1, is indicated by the arrow. The schematic shows substrates placed as deduced from the major products. Individual cleavage frequencies are indicated above the bonds.

lation was observed only for [T212W]AMY1 that formed 3% PNPNG<sub>6</sub> at 35% PNPNG<sub>5</sub> consumption. This may be associated with its improved affinity, since the double mutant Y105A/T212W apparently did not catalyze transglycosylation and had higher  $K_m$  for oligosaccharide (Table I).

**Docking of Maltododecaose to AMY1 and AMY2**—Maltododecaose complexes were computed to get a structural basis for interpretation of the substrate preferences of AMY1 mutants and the suggested presence of different binding modes. Earlier models showed for some  $\alpha$ -amylases two types of partially superimposed maltododecaose docking solutions (S1 and S2) reflecting bifurcation near the glycone binding subsites -3/-4. While fungal and animal  $\alpha$ -amylases preferred S1, AMY2 preferred the S2 type (12). The present thorough calculation of maltododecaose complexes in addition led to a novel solution, S3, that deviated from S2 beyond the aglycone subsite +3 (Figs. 3 and 4, A and C; Table II). The energy of S1<sub>AMY1</sub>, S2<sub>AMY1</sub>, and S3<sub>AMY1</sub> was 37, 3, and 13 kcal  $\times$  mol<sup>-1</sup>, respectively, relative to S2<sub>AMY2</sub>, the most favorable solution set to 0 kcal  $\times$  mol<sup>-1</sup>, while S1<sub>AMY2</sub> and S3<sub>AMY2</sub> had 48 and 18 kcal  $\times$  mol<sup>-1</sup>, respectively. The smaller mutual energy differences for the three AMY1 solutions suggested that multiple binding modes are populated to a greater extent for AMY1 than AMY2. Moreover, the similar docking energies of solutions for AMY1 and AMY2 indicated high resemblance of the active sites de-

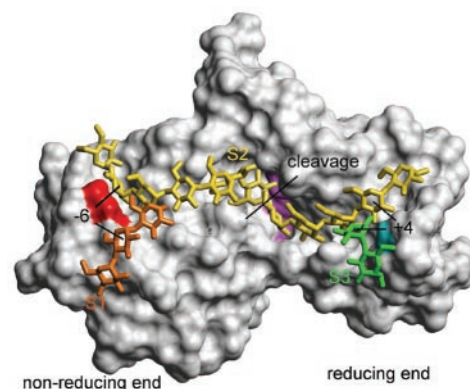


FIG. 3. Maltododecaose docking solutions in the substrate binding area of AMY1. Truncated AMY1 (see “Experimental Procedures” and Ref. 25) is represented by the Connolly surface. Maltododecaose in the S2 solution is shown in yellow, glucose rings in orange and green correspond to glycone and aglycone parts of the S1 and S3 solutions, respectively. The surface of the three catalytic acids Asp<sup>180</sup>, Glu<sup>205</sup>, Asp<sup>291</sup> is in pink and of Tyr<sup>105</sup> and Trp<sup>299</sup> in brown and blue, respectively. These latter two residues clearly delimit furrows at outer regions of the binding area.

spite distinct differences in structure and function.

The energy map of  $\alpha$ -1,4 disaccharide dihedral angles ( $\varphi$ ,  $\psi$  = O5'-C1'-O4-C4, C1'-O4-C4-C5) includes contiguous regions A ( $\varphi$ ,  $\psi$ ; 56, -151); B (114, -133); and C (133; -108); while E (85, 84) (46) is separate. B is like a single helix (SH) (67) and a nearby region corresponds to a single chain in a double helix (DH) found in A and B type starch (68). Repeated A, SH, and DH generate left helices, which C or E disrupt (46). The present S1, S2, and S3 solutions share disaccharide conformations with those compiled for oligosaccharides bound in different GH-H crystal structures (28). S2<sub>AMY1</sub> adopts mainly the more stable DH with a single break (C: 118, -106) between subsites +2 and +3. In S1<sub>AMY1</sub> kinks at subsites -3 (C: 156, -107) and -5 (C: 147, -106) direct the three outer residues (orange in Fig. 3) to another crevice branch. Similarly, in S3<sub>AMY1</sub> E (91, 116) at subsite +3 turns the chain (green in Fig. 3) and C at subsites +4 (158, -97) and +5 (146, -108) prevents left helical propagation. In S1 and S3 the orientation of glucose O6 at subsites -4 and +3 is compatible with a branch accommodated at outer subsites according to S2. Both mutational changes at outer subsites and conformational differences between substrates will influence the relative occupancy of S1, S2, and S3.

**Partial Binding Energy Contributions Calculated for Individual Subsites**—The distribution of intermolecular binding energies at individual subsites (see “Experimental Procedures”) in S1, S2, and S3 (Table II) are comparable with the subsite map, except for its low affinity at subsite +3 (5). This difference may stem from shorter oligosaccharides being used in subsite mapping. S2<sub>AMY1</sub> displays a regular pattern of strong and medium energies for subsites -7, -6, -2, -1, +1, +2, +3 and -5, -4, -3, +4, +5, respectively, and lacks weak subsites (Table II). Most remarkably, all the high energy subsites include stacking interactions, listed in the same order, with Tyr<sup>98</sup>, Tyr<sup>105</sup>, Tyr<sup>52</sup>, Phe<sup>181</sup>, Trp<sup>207</sup>, and Trp<sup>299</sup> (Fig. 4A). The high affinity subsite -6 in S2<sub>AMY1</sub> contains Val<sup>47</sup>, Cys<sup>95</sup>, Ala<sup>96</sup>, Tyr<sup>105</sup>, Tyr<sup>131</sup>, and Ala<sup>146</sup> (25), which are conserved in AMY2 except Cys<sup>95</sup><sub>AMY1</sub> corresponding to Thr<sup>94</sup><sub>AMY2</sub>, which has an important role in substrate binding (39). Subsites -4 through -7 in S1<sub>AMY1</sub> have lower energy and no stacking (Table II and Fig. 4, A and B). The lower stability of S1<sub>AMY1</sub> is in addition explained by fewer charged hydrogen bonds with substrate at subsites -6 and -7 (Table II, A) and rotation of the Tyr<sup>105</sup> side chain (Fig. 4, A and B).

The new solutions S3<sub>AMY1</sub> and S3<sub>AMY2</sub> have intermediate

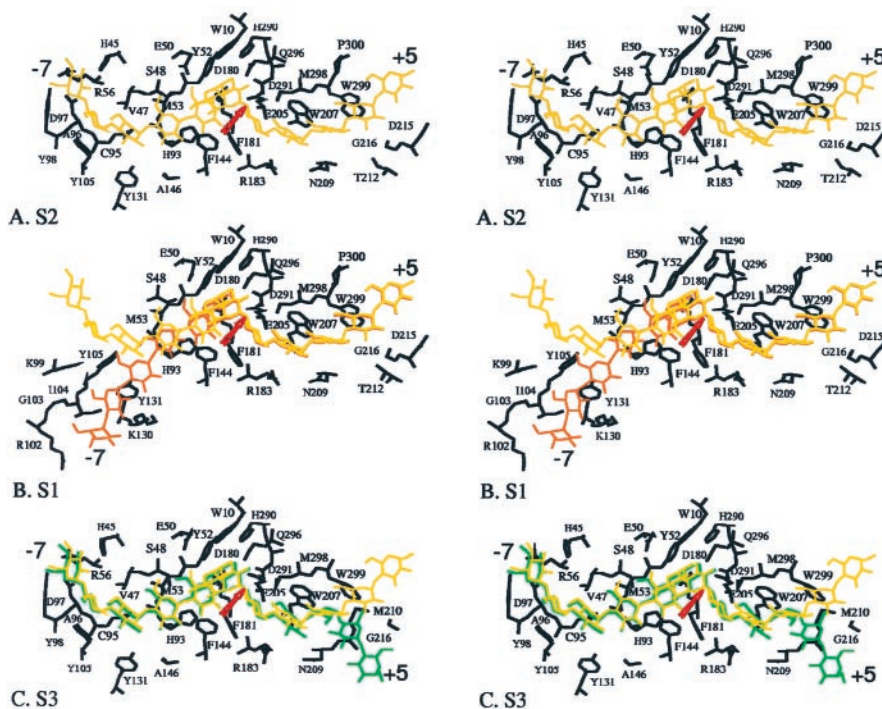


FIG. 4. Stereoview of AMY1/maltododecaose docking solutions. From the top the solutions S2 (A), S1 (B), and S3 (C) show maltododecaose spanning subsites -7 through +5. AMY1 residues important in binding (Table II) are shown. Tyr<sup>98</sup>, Tyr<sup>105</sup>, Tyr<sup>52</sup>, Phe<sup>181</sup>, Trp<sup>207</sup>, Trp<sup>299</sup> participate in stacking interactions. The S2 solution is superimposed (in yellow) in B and C. The arrow indicates the cleavage site.

energy to S2 and S1. S3<sub>AMY1</sub> lacks stacking onto Trp<sup>299</sup> at subsite +3 (see Fig. 4C; Table II) and compared with the AMY2 docking solutions, S3<sub>AMY1</sub> is more favorable than S2<sub>AMY1</sub> at subsites +1 and +2, and less favorable at subsite +3 (Table II, A and B). Similarly, S2<sub>AMY2</sub> has higher energy than S3<sub>AMY2</sub> for subsite +3 and the AMY2 mimic [T212Y]AMY1 therefore may have gained its substantially enhanced affinity for amylose DP17 (Table I) by adopting S2<sub>AMY1</sub>. The poor affinity of Y105A for amylose DP17 is not compensated in the [Y105A/T212(Y/W)]AMY1 despite the otherwise favorable T212(Y/W) mutation. One can therefore speculate that in the double mutants amylose DP17 adopts S3<sub>AMY1</sub> for the aglycone in combination with S1<sub>AMY1</sub> for the glycone, Y105A diminishing the energy difference of S1 and S2 (Table II A). This latter and presumably least energetically favorable solution agreed with an important loss in transition state stabilization for amylose DP17 by the double mutants (Table I).

#### DISCUSSION

**$\alpha$ -Amylase Substrate Interactions**—Subtle structural changes of AMY1 involving aromatic side-chains far from the catalytic site have large, diverse effects on oligosaccharide, maltodextrin, and insoluble polysaccharide substrates. Aromatic stacking in carbohydrate-binding proteins is well known (26, 27, 49) and is important throughout GH-H (9–11, 21, 28, 63). CH at positions 1, 2, and 4 on the A face of glucose rings form a cluster of stronger contact to the outer curvature in the maltodextrin helix than CH groups at positions 3 and 5 of the B face (27). In S2<sub>AMY1</sub> Tyr<sup>52</sup>, Tyr<sup>98</sup>, Tyr<sup>105</sup>, and Phe<sup>181</sup> thus stack onto glucose A faces at subsites -1, -7, -6, and +1, and Trp<sup>207</sup> and Trp<sup>298</sup> onto B faces at subsites +2 and +3. No stacking occurred at subsites -7, -6, and +3 in the two less favorable solutions S1<sub>AMY1</sub> and S3<sub>AMY1</sub>. The modeled AMY1/maltododecaose complexes do not account for hydrolysis of larger substrates that most probably have distant, additional interactions between enzyme and substrate perhaps with other parts of the substrate molecule. Starch thus binds to at least one (42) of two surface sites in AMY1 (10, 31). Moreover, binding of oligosaccharides or other substrate molecules at such secondary site(s) may induce long range effects on accom-

modation of substrates at the active site.

**Relation between Mutant Activity and Modeled AMY1/Maltododecaose: Glycone Binding Region**—Overall maltododecaose docking to mutants (not shown) resembled that of wild-type AMY1. Starch and amylose DP17 can span the entire binding crevice, while Cl-PNPG<sub>7</sub> and PNPG<sub>5-7</sub> probe the outer subsites -6 and +4 individually. The enzymatic properties of [Y105(F/W)]AMY1 support stacking at subsite -6 according to the S2 docking solution. Consistent with reduced activity on starch of [Y105W]AMY1, the indole ring in the modeled maltododecaose complex points toward the same part of the binding cleft (not shown) as Tyr<sup>105</sup> in wild type. Y105F lacked the Tyr<sup>105</sup>  $\gamma$ OH-glucose O6 hydrogen bond at subsite -6 and lost affinity only for Cl-PNPG<sub>7</sub>. PNPG<sub>6</sub> accordingly binds at subsites -5 through +2, rather than -6 through +1 as in Y105W and wild-type AMY1. This behavior agrees with Y105F having increased activity for starch, suggesting, together with the elevated activity of [Y105A]AMY1, that stacking at subsite -6 in S2 adversely affects activity for starch. S1 seems preferred for Y105(A/F) over S2 in hydrolysis of starch. In contrast, reduced and maintained affinity, respectively, by Y105A and Y105(Y/W) for amylose DP17 suggested S2 to be predominant with short chain linear maltodextrins. Accordingly modeling using Y105A indicated no energy gain for S1, which is the least favorable wild-type AMY1/maltododecaose solution, supporting the interpretation that S2 type conformation is maintained for bound amylose DP17. Thus S1 is speculated to be adopted primarily by polysaccharides. Y105A, however, may still affect S1 through van der Waal's contacts between its backbone oxygen and the ring of Tyr<sup>131</sup> as deduced from the structure (not shown). Since Tyr<sup>131</sup><sub>AMY1</sub> is close to glucose bound at subsite -5, perhaps Y105A has a different impact than wild-type Tyr<sup>105</sup> on S1. The subsite -5 mutant C95A AMY1 doubled activity on starch (39) providing support for S2<sub>AMY1</sub> counteracting starch hydrolysis, since C95 is only involved with substrate in S2<sub>AMY1</sub> (Table II). C95A might perturb accommodation of a helical  $\alpha$ -1,4-glucoside chain in S2<sub>AMY1</sub> for shorter substrates reflected in 5- and 20-fold loss of affinity for amylose DP17 and Cl-PNPG<sub>7</sub>, respectively. Starch, however, with less

TABLE II  
Calculated binding energies and interacting residues in maltododecaose docked to AMY1 (A) and AMY2 (B)

Subsite	S2 solution				S1 solution (upper part)			
	Residues involved (relative binding energy) <sup>a</sup>	Stacking	Main binding mode	vdW	Residues involved (relative binding energy)	Stacking	Main binding mode	vdW
	<i>kcal × M<sup>-1</sup></i>							
<b>A. AMY1</b>								
-7	H45, R56, D97, Y98(-32)	Y98(-11)	H45, R56(-8)	(-13)	R102, G103, I104, K130(-17)		R102(-4)	(-13)
-6	V47, C95, A96, D97, Y105(-24)	Y105(-10)	A96, D97(-7)	(-7)	K99, G103, I104, Y105, K130, Y131(-21)		G103, Y131(-4)	(-17)
-5	V47, M53, C95, Y131(-13)		Y131(-8)	(-5)	Y105, K130(-11)		Y105(-4)	(-7)
-4	V47, S48, M53, A146(-11)		S48(-4)	(-7)	Y105(-6)		Y105(-5)	(-1)
-3	S48, E50, F144(-11)		E50(-3)	(-8)	S48, E50, F144(-16)		S48, E50(-8)	(-8)
-2	W10, S48, Y52, M53, H93, F144, D291, Q296(-28)		Y52, D296(-10)	(-18)	W10, S49, Y52, M53, H93, F144, D291, Q296(-27)		Y52, H93, Q296(-8)	(-19)
-1	Y52, H93, F144, D180, F181, E205, H290, D291(-36)	Y52(-3)	H93, D180, E205, D291(-18)	(-15)				
+1	F181, R183, E205, W207, D291(-27)	F181(-7)	R183, D291(-10)	(-10)	F181, R183, E205, W207, D291(-34) <sup>b</sup>	F181(-9) <sup>b</sup>	H205, W207, D291(-12) <sup>b</sup>	(-13) <sup>b</sup>
+2	R183, W207, N209, D291, M298(-22)	W207(-9)	R183, N209(-7)	(-6)	R183, W207, N209, D291, M298(-27) <sup>b</sup>	W207(-11) <sup>b</sup>	R183, N209(-10) <sup>b</sup>	(-6) <sup>b</sup>
+3	W207, N209, M298, W299(-22)	W299(-10)	W207, M298(-9)	(-3)	W207, D208, M210, M298, W299(-22) <sup>b</sup>		W207, M210, M298(-14) <sup>b</sup>	(-8) <sup>b</sup>
+4	D215, G216, M298, W299(-16)		D215, G216(-6)	(-10)	T212, G216, W299(-13) <sup>b</sup>		G216, W299(-10) <sup>b</sup>	(-3) <sup>b</sup>
+5	K217, N255, A256, W299, P300(-18)		W299, P300(-8)	(-10)	T212, G213, G214, D215, G216(-13) <sup>b</sup>			(-13) <sup>b</sup>
<b>B. AMY2</b>								
-7	Q44, V46, E96, H97(-29)	Y104(-12)	R55, E96, H97(-11)	(-18)	R101, I103, P129(-14)		R101(-4)	(-10)
-6	V46, T94, A95, E96, Y104(-30)		T94, A95, E96(-10)	(-8)	G102, I103, P129(-11)		G102(-4)	(-7)
-5	V46, M52, Y130(-13)		Y130(-8)	(-5)	Y130(-9)		Y130(-6)	(-3)
-4	V46, A47, M52(-9)		V46(-3)	(-6)	M52(-1)			(-1)
-3	A47, F143(-5)			(-5)	A47, M52, F143(-6)			(-6)
-2	W9, A47, Y51, F143, D289, Q294(-28)		Y51, Q294(-9)	(-19)	W9, A47, Y51, M52, H92, F143, D289, Q294(-28)		Y51, Q294(-9)	(-19)
-1	W9, Y51, H92, D179, F180, F204, H288, D289(-35)	Y51(-3)	H92, D179, E204, D289(-17)	(-15)				
+1	F180, K182, E204, W206, D289(-29)	F180(-7)	D289(-8)	(-14)	F180, K182, E204, W206, D289(-31) <sup>b</sup>	F180(-8) <sup>b</sup>	W206, D289(-8) <sup>b</sup>	(-15) <sup>b</sup>
+2	K182, W206, S208, M296(-19)	W206(-10)	W206, S208(-4)	(-5)	K182, W206, S208(-18) <sup>b</sup>	W206(-9) <sup>b</sup>	K182, S208(-7) <sup>b</sup>	(-2) <sup>b</sup>
+3	W206, S208, Y211, M296, W297(-31)	W297(-9)	S208, Y211, M296(-12)	(-10)	K182, W206, S208, D289, M296(-23) <sup>b</sup>	Y211(-8) <sup>b</sup>	S208, M296(-11) <sup>b</sup>	(-12) <sup>b</sup>
+4	D214, G215, M296, W297, P298(-15)		D214, G215(-7)	(-8)	Y211, G215, W297(-13) <sup>b</sup>		G215(-3) <sup>b</sup>	(-2) <sup>b</sup>
+5	D214, K216, N253, Y254, W297, P298(-23)		214, W297, P298(-10)	(-13)	Y211, G212, G213, D214, G215(-19) <sup>b</sup>		G212(-3) <sup>b</sup>	(-16) <sup>b</sup>

<sup>a</sup> For calculation of energies see "Experimental Procedures."

<sup>b</sup> S3 solution.

regular propagation probably adopted S1. The activity of the AMY2 mimic [C95T]AMY1 resembled that of C95A and agreed with Thr<sup>94</sup><sub>AMY2</sub> contributing less docking energy than Cys<sup>95</sup><sub>AMY1</sub> at subsites -5 and -6 (Table II). Asp<sup>97</sup><sub>AMY1</sub> at subsite -6 in S2<sub>AMY1</sub> (Table II) is also functionally important, and the AMY2 mimic D97E AMY1 reduced affinity for Cl-PNPG<sub>7</sub> and amylose DP17 4- and 2-fold, respectively (43).

The S1, S2, and S3 AMY1/maltododecaose are most helpful in understanding mutant properties, although the computed binding energies of the three docking solutions differed from those derived from the kinetics. Thus loss in transition state stabilization energy for Y105A acting on amylose DP17 was 1.0 kcal  $\times$  mol<sup>-1</sup> according to  $\Delta\Delta G = -RT\ln [(k_{\text{cat}}/K_m)_{\text{mutant}}/(k_{\text{cat}}/K_m)_{\text{parent}}]$  (69). Considering T212Y and T212W as parents of the double mutants,  $\Delta\Delta G$  was 2.3 and 1.4 kcal  $\times$  mol<sup>-1</sup>, respectively. In relation to Cl-PNPG<sub>7</sub> an estimate of  $(k_{\text{cat}}/K_m)_{\text{mutant}}/(k_{\text{cat}}/K_m)_{\text{parent}} > 100$  for Y105A gave to  $\Delta\Delta G > 2.8$  kcal  $\times$  mol<sup>-1</sup> and using T212Y and T212W as parents both gave  $\Delta\Delta G = 1.6$  kcal  $\times$  mol<sup>-1</sup>. These losses are smaller than the calculated energy of 10 kcal  $\times$  mol<sup>-1</sup> corresponding to loss of stacking for Y105A in S2<sub>AMY1</sub> at subsite -6 (Table II A) or than the difference between S1<sub>AMY1</sub> and S2<sub>AMY1</sub> of 34 kcal  $\times$  mol<sup>-1</sup>. The discrepancy emphasizes that smaller energy differences were realized in enzyme hydrolysis than by comparison of computed docking energies of mutants and wild type. This might stem from different principles inherent to the two approaches used to assess energy losses, the different substrate size of DP12 and DP17, or both. It may also reflect that as anticipated in reality multiple modes, rather than one specific, are employed for a particular substrate and AMY1 mutant or wild-type interaction.

**Aglycone Binding Region**—AMY2 mimicry by T212Y AMY1 increased activity for amylose DP17 almost 4-fold and maintained wild-type kinetics for Cl-PNPG<sub>7</sub>. Since AMY2, however, has a 4-fold higher  $k_{\text{cat}}$  than AMY1 for amylose DP17, but also a 3-fold higher  $K_m$  (65), the T212Y mimic was superior to AMY2. This suggested S2-associated improvement of outer aglycone interactions in the AMY2 mimic, since wild-type S3<sub>AMY1</sub> and S2<sub>AMY1</sub> have similar, but S2<sub>AMY2</sub> has higher energy than S3<sub>AMY2</sub>. [T212Y]AMY1 thus demonstrates potential for ameliorating AMY2 by replacement of the corresponding Tyr<sup>211</sup>. The related natural isozyme specificity difference may be important in starch mobilization reactions in the germinating seed.

Introduction of aromatic groups at subsite +4 in [T212(Y/W)]AMY1 reduced activity for starch. It appears therefore that aromatic groups at outermost subsites might trap polysaccharide substrates in conformations less suitable for catalysis. Still [T212(P/Y/W)]AMY1 motivated Thr<sup>212</sup> replacement to selectively improve activity on soluble substrates and S3<sub>AMY1</sub> and S2<sub>AMY1</sub> seemed equally applicable for T212P AMY1/maltododecaose. Whereas T212P maintained AMY1 wild-type oligosaccharide action patterns, especially T212W, but also [T212Y]AMY1, shifted productive oligosaccharide binding position toward the aglycone binding area, conceivably by strengthened contacts at outer subsites in S2.

**Modification at Both Outer Binding Regions**—The substrate preferences of Y105A/T212(Y/W) supported the presence of multiple substrate binding modes.  $K_m$  decreased only for all three substrates when Y105A and T212W were combined, while combination of Y105A with the AMY2 mimic T212Y were less active indicating room for improvement of wild-type AMY2 by mutagenesis. Y105A/T212W only on Cl-PNPG<sub>7</sub> showed special advantage over Y105A probably due to aglycone sliding. Double mutation at subsites -6 and +4 resulted in kinetic

parameters for Cl-PNPG<sub>7</sub> hydrolysis, that were intermediate to those of single mutants. Y105A/T212(Y/W) showed an additive effect of single mutants that greatly changed oligosaccharide action patterns. T212(Y/W) thus ameliorated poor activity of Y105A by further strengthening the enhanced aglycone binding mode and transition state stabilization. Based on substrate consumption rates (not shown), [Y105A]AMY1 decreased activity substantially for PNPG<sub>7</sub> and PNPG<sub>6</sub>, but as expected retained wild-type level for PNPG<sub>5</sub> that cannot utilize subsite -6. Y105A/T212W had similarly low activity for PNPG<sub>7</sub>, but wild-type level and higher for PNPG<sub>6</sub> and PNPG<sub>5</sub>, respectively, in agreement with improved affinity and increased  $k_{\text{cat}}/K_m$  toward Cl-PNPG<sub>7</sub> for [T212W]AMY1. Y105A/T212Y, however, reduced turnover of PNPG<sub>5-7</sub> probably due to loss of affinity. This diversity of structurally very similar AMY1 mutants emphasized large flexibility in enzyme-substrate interactions in response to subtle variation in intermolecular contacts and illustrated the potential of specificity engineering at outer subsites in GH-H.

Inferior starch hydrolysis of Y105A/T212Y suggested that S1 was combined with S3. Amylose DP17 and starch both span the two exterior subsites and loss of co-operation between them in substrate complexes might lower  $k_{\text{cat}}$  and  $k_{\text{cat}}/K_m$  for double compared with single mutants. The simultaneous structural change of terminal substrate anchor points in the binding crevice thus might hamper transition state stabilization of some substrates.

**Branched Maltodextrins**—The present maltododecaose docking neglected simultaneous filling of the two binding crevices by branched substrates. Tyr<sup>105</sup> was expected to be critical for subsites -4 through -7 in S2<sub>AMY1</sub> binding of branches with the main chain binding according to S1<sub>AMY1</sub> (70). Because homogenous branched substrates of a certain size are not available information on enzymatic hydrolysis lags behind. The 6''-maltotriosyl-maltohexaose, however, was hydrolyzed 30 times slower than maltopentaose by AMY1 and product analysis indicated the  $\alpha$ -1,4;1,6-disubstituted glucose to bind at subsite +2 (39). The low activity in combination with the product structure support that the subsite -4 binding could be applied of the branch point as proposed by modeling, which, however was not compatible with the structure of the available nonasaccharide.

**Substrate Preference Engineering**—Certain mutants at subsites -5, -3, -2, -1, +1, and +2 had retained or increased parent enzyme activity toward starch and reduced activity for shorter substrates and *vice versa* (30, 39-41). Wild-type AMY1 was not optimal for starch interactions, and [Y105A/T212(Y/W)]AMY1 preferred starch for short substrates more strongly than wild type. An estimated >100-fold preference for starch of Y105A compared with wild-type AMY1 makes the mutant a candidate for controlled starch degradation accompanied by slow attack on the produced oligosaccharides. Engineered outer subsites thus radically alters substrate specificity and product profiles. AMY1 has about 5-fold higher affinity for oligosaccharides and maltodextrins than AMY2 (6, 7) and 7 (Gln<sup>44</sup>, Ala<sup>47</sup>, Thr<sup>94</sup>, Glu<sup>96</sup>, Lys<sup>182</sup>, Ser<sup>208</sup>, and Tyr<sup>211</sup>) of the 28 amino acid residues that directly bind substrate via aromatic stacking, hydrogen bond, and van der Waals' interactions in S2<sub>AMY2</sub> changed in AMY1 to His<sup>45</sup>, Ser<sup>48</sup>, Cys<sup>95</sup>, Asp<sup>97</sup>, Arg<sup>183</sup>, Asn<sup>209</sup>, and Thr<sup>212</sup> (33, 38). Three available AMY2 mimics, C95T (39), D97E (43), R183K (40), but not [T212Y]AMY1 (present work) increased  $K_m$  for amylose DP17 indicating implication in the isozyme difference (37). Such mutants constitute a source of information for guiding rational design of enzymatic properties of AMY1. This insight might be exploited to engineer related GH-H enzymes. Obviously it is of great interest to explore

Thr<sup>212</sup> and other selected positions in AMY1 by saturation mutagenesis.

**Roles of Distant Subsites in Other Glycoside Hydrolases**—Multiple substrate binding modes controlled by subtle enzyme structural features may be more common in polysaccharide degrading enzymes than yet realized and possibly occur as long range coordinated interactions in polysaccharide synthases (71). Outer subsites, however, are examined only in a few polysaccharide hydrolases. Thus mutation of a gate-controlling tryptophan at subsite +4 in cellulase Cel6A from *Trichoderma reesei* (72) highlighted its key role in degradation of crystalline cellulose. Furthermore, in Cel6A from *Humicola insolens* the groove-type topology of the binding site was altered to a tunnel by a polypeptide loop cover affecting the outer subsites and polysaccharide-enzyme interactions (73, 74). A different type of long range effect was demonstrated for glucoamylase by combined substrate and enzyme engineering, where a charged enzyme-substrate hydrogen bond at subsite +1 controlled critical transition state stabilizing interactions at subsite -1 (75, 76). Finally, a mutant of E43 at subsite -2 in endo-xylanase from *Pseudomonas cellulosa* provided evidence for differential binding of short and long substrates by distinct mechanisms controlled at a distance of the catalytic site (77). This latter behavior was reminiscent of [Y105A]AMY1 that lost and gained activity, respectively, for oligosaccharides and starch. From GH-H, mutants in subsite -6 of CGTase decreased  $k_{cat}$  for the three transglycosylation reactions; cyclodextrin formation; disproportionation; and coupling, but retained hydrolytic activity (45). Subsite -6 was concluded to regulate induced fit of the catalytic site, which was critical for transglycosylation (45). The work on CGTase emphasized that rational engineering at outer subsites is a realistic approach to achieve desirable properties. Future protein engineering (15) of amylolytic enzymes by *e.g.* structure-guided directed evolution and rational design can exploit the knowledge gained in subsite engineering to meet specificity requirements and to improve insight into enzyme-substrate relationships (48).

#### CONCLUSION

Aromatic engineering at outer subsites -6 and +4 in barley  $\alpha$ -amylase 1 (AMY1) greatly modified kinetic properties and action patterns on different substrates without loss of the wild-type level of catalytic activity. Three partially superimposed and energetically different AMY1/maltododecaose docking solutions were calculated and properties of the mutants at outer subsites -6 and +4 were compatible with change of the area of accommodation of the substrate chain at a distance of 3–4 subsites from the catalytic site. Thus loss of wild-type stacking onto substrate at subsite -6 in [Y105A]AMY1 and introduction of substrate hydrogen bonding and stacking at subsite +3 and +4 in [T212(Y/W)]AMY1, the AMY2 Tyr<sup>211</sup> mimic, were supported. Elevated activity for starch and decreased activity for oligosaccharides of Y105A suggested that polysaccharide binds according to the energetically less favorable S1 AMY1/maltododecaose solution. Since [T212(Y/W)]AMY1 increased activity for maltodextrins, but lost activity for starch, both natural (Tyr<sup>105</sup>) and engineered (T212(Y/W)) aromatic groups at outermost binding subsites might trap polysaccharide in conformations unfavorable for hydrolysis. Fine adjustment, however, is possible in double mutants, Y105A/T212W regaining activity on starch, but losing activity on the maltodextrin. Both positions Tyr<sup>105</sup> and Thr<sup>212</sup> give room for additional mutational improvement of enzymatic performance, *e.g.* through saturation mutagenesis. Although reliable design of properties cannot be anticipated from the present limited number of mutants the gained experience is applicable in engineering of outer subsites in related GH-H members. Flexibly modulated activity could be

further developed by gene shuffling by including selected mutants as parents.

**Acknowledgments**—We thank Sidsel Ehlers, Annette Gajhede, Lone Sørensen, Pia Breddam, Ib Svendsen, and the late Bodil Corneliussen for excellent technical assistance.

#### REFERENCES

1. Yamamoto, T. (1995) *Enzyme Chemistry and Molecular Biology of Amylases and Related Enzymes*, The Amylase Research Society of Japan, CRC Press, Boca Raton, FL
2. Robyt, J. F., and French, D. (1970) *J. Biol. Chem.* **245**, 3917–3927
3. Suganuma, T., Matsuno, R., Ohnishi, M., and Hiromi, K. (1978) *J. Biochem. (Tokyo)* **84**, 293–316
4. Matsui, I., Ishikawa, K., Matsui, E., Miyairi, S., Fukui, S., and Honda, K. (1991) *J. Biochem. (Tokyo)* **109**, 566–569
5. Ajandouz, E. H., Abe, J., Svensson, B., and Marchis-Mouren, G. (1992) *Biochim. Biophys. Acta* **1159**, 193–202
6. MacGregor, A. W., Morgan, J. E., and MacGregor, E. A. (1992) *Carbohydr. Res.* **227**, 301–313
7. MacGregor, E. A., MacGregor, A. W., Macri, L. J., and Morgan, J. E. (1994) *Carbohydr. Res.* **257**, 249–268
8. Brayer, G. D., Sidhu, G., Maurus, R., Rydberg, E. H., Braun, C., Wang, Y., Nguyen, N. T., Overall, C. M., and Withers, S. G. (2000) *Biochemistry* **39**, 4778–4791
9. Qian, M., Haser, R., Buisson, G., Duee, E., and Payan, F. (1994) *Biochemistry* **33**, 6284–6294
10. Kadziola, A., Søgaard, M., Svensson, B., and Haser, R. (1998) *J. Mol. Biol.* **278**, 205–217
11. Fujimoto, Z., Takase, K., Doui, N., Momma, M., Matsumoto, T., and Mizuno, H. (1998) *J. Mol. Biol.* **277**, 393–407
12. André, G., and Tran, V. (1999) in *Recent Advances in Carbohydrate Bioengineering* (Gilbert, H. J., Davies, G. J., Henrissat, B., and Svensson, B., eds) pp. 165–174, The Royal Society of Chemistry, Cambridge
13. Dauter, Z., Dauter, M., Brzozowski, A. M., Christensen, S., Borchert, T. V., Beier, L., Wilson, K. S., and Davies, G. J. (1999) *Biochemistry* **38**, 8385–8392
14. Brzozowski, A. M., Lawson, D. M., Turkenburg, J. P., Bisgaard-Frantzen, H., Svendsen, A., Borchert, T. V., Dauter, Z., Wilson, K. S., and Davies, G. J. (2000) *Biochemistry* **39**, 9099–9107
15. MacGregor, E. A., Janecek, S., and Svensson, B. (2001) *Biochim. Biophys. Acta* **1546**, 1–20
16. Uitdehaag, J. C., van der Veen, B. A., Dijkhuizen, L., Elber, R., and Dijkstra, B. W. (2001) *Proteins* **43**, 327–335
17. Kadziola, A., Abe, J., Svensson, B., and Haser, R. (1994) *J. Mol. Biol.* **239**, 104–121
18. Henrissat, B. (1991) *Biochem. J.* **280**, 309–316
19. Janecek, S. (2002) *Biologia, Bratislava* **57**, 29–41
20. Machius, M., Vértessy, L., Huber, R., and Wiegand, G. (1996) *J. Mol. Biol.* **260**, 409–421
21. Brzozowski, A. M., and Davies, G. J. (1997) *Biochemistry* **36**, 10837–10845
22. Uitdehaag, J. C., Mosi, R., Kalk, K. H., van der Veen, B. A., Dijkhuizen, L., Withers, S. G., and Dijkstra, B. W. (1999) *Nat. Struct. Biol.* **6**, 432–436
23. Uitdehaag, J. C., Kalk, K. H., Der Veen, B. A., Dijkhuizen, L., and Dijkstra, B. W. (1999) *J. Biol. Chem.* **274**, 34868–34876
24. Uitdehaag, J. C., van Alebeek, G. J., Der Veen, B. A., Dijkhuizen, L., and Dijkstra, B. W. (2000) *Biochemistry* **39**, 7772–7780
25. André, G., Buleon, A., Haser, R., and Tran, V. (1999) *Biopolymers* **50**, 751–762
26. Vyas, N. K. (1991) *Curr. Opin. Struct. Biol.* **1**, 732–740
27. Quicho, F. A., Spurlino, J. C., and Rodseth, L. E. (1997) *Structure* **5**, 997–1015
28. Przylas, I., Terada, Y., Fujii, K., Takaha, T., Saenger, W., and Sträter, N. (2000) *Eur. J. Biochem.* **267**, 6903–6913
29. Aghajari, N., Feller, G., Gerday, C., and Haser, R. (1998) *Protein Sci.* **7**, 564–572
30. Gottschalk, T. E., Tull, D., Aghajari, N., Haser, R., and Svensson, B. (2001) *Biochemistry* **40**, 12844–12854
31. Robert, X., Haser, R., Gottschalk, T. E., Ratajczak, F., Driguez, H., Svensson, B., and Aghajari, N. (2003) *Structure* **11**, 973–984
32. Janecek, S., Svensson, B., and MacGregor, E. A. (2003) *Eur. J. Biochem.* **270**, 635–645
33. Rogers, J. C. (1985) *J. Biol. Chem.* **260**, 3731–3738
34. Jones, R. L., and Jacobsen, J. V. (1991) *Int. Rev. Cytol.* **126**, 49–88
35. Rodenburg, K. W., Juge, N., Guo, X.-J., Søgaard, M., Chaix, J.-C., and Svensson, B. (1994) *Eur. J. Biochem.* **221**, 277–284
36. Bertoft, E., Andtfolk, C., and Kulp, S.-E. (1984) *J. Inst. Brew.* **90**, 298–302
37. Søgaard, M., and Svensson, B. (1990) *Gene* **94**, 173–179
38. Rogers, J. C., and Milliman, C. (1983) *J. Biol. Chem.* **258**, 8169–8174
39. Mori, H., Bak-Jensen, K. S., Gottschalk, T. E., Motawia, M. S., Damager, I., Møller, B. L., and Svensson, B. (2001) *Eur. J. Biochem.* **268**, 6545–6558
40. Matsui, I., and Svensson, B. (1997) *J. Biol. Chem.* **272**, 22456–22463
41. Mori, H., Bak-Jensen, K. S., and Svensson, B. (2002) *Eur. J. Biochem.* **269**, 5377–5390
42. Søgaard, M., Kadziola, A., Haser, R., and Svensson, B. (1993) *J. Biol. Chem.* **268**, 22480–22484
43. Jensen, M. T., Gottschalk, T. E., and Svensson, B. (2003) *J. Cereal Sci.* **38**, 289–300
44. Nitta, Y., Mizushima, M., Hiromi, K., and Ono, S. (1971) *J. Biochem. (Tokyo)* **69**, 567–576
45. Leemhuis, H., Uitdehaag, J. C., Rozeboom, H. J., Dijkstra, B. W., and Dijkhuizen, L. (2002) *J. Biol. Chem.* **277**, 1113–1119
46. André, G., Buleon, A., Tran, V., Vallée, F., Juy, M., and Haser, R. (1996) *Biopolymers* **39**, 737–751

47. André, G., Buléon, A., Juy, M., Aghajari, N., Haser, R., and Tran, V. (1999) *Biopolymers* **49**, 107–119
48. Nielsen, J. E., and Borchert, T. V. (2000) *Biochim. Biophys. Acta* **1543**, 253–274
49. Quiócho, F. A. (1993) *Biochem. Soc. Trans.* **21**, 442–448
50. Boel, E., Brady, L., Brzozowski, A. M., Derewenda, Z., Dodson, G. G., Jensen, V. J., Petersen, S. B., Swift, H., Thim, L., and Woldike, H. F. (1990) *Biochemistry* **29**, 6244–6249
51. Machius, M., Declerck, N., Huber, R., and Wiegand, G. (1998) *Structure* **6**, 281–292
52. Parsiegla, G., Schmidt, A. K., and Schulz, G. E. (1998) *Eur. J. Biochem.* **255**, 710–717
53. Kamitori, S., Kondo, S., Okuyama, K., Yokota, T., Shimura, Y., Tonozuka, T., and Sakano, Y. (1999) *J. Mol. Biol.* **287**, 907–921
54. Juge, N., Andersen, J. S., Tull, D., Roepstorff, P., and Svensson, B. (1996) *Protein Expr. Purif.* **8**, 204–214
55. Sogaard, M., Andersen, J. S., Roepstorff, P., and Svensson, B. (1993) *Bio/Technology* **11**, 1162–1165
56. Landt, O., Grunert, H. P., and Hahn, U. (1990) *Gene (Amst.)* **96**, 125–128
57. Sambrook, J., Fritsch, E. F., and Maniatis, T. (1989) *Molecular Cloning: A Laboratory Manual*, 2nd Ed., Cold Spring Harbor Laboratory, Cold Spring Harbor, NY
58. Sanger, F., Nicklen, S., and Coulson, A. R. (1977) *Proc. Natl. Acad. Sci. U. S. A.* **74**, 5463–5467
59. Svensson, B., Mundy, J., Gibson, R. M., and Svendsen, I. (1985) *Carlsberg. Res. Commun.* **50**, 15–22
60. Andersen, J. S., Sogaard, M., Svensson, B., and Roepstorff, P. (1994) *Biol. Mass Spectrom.* **23**, 547–554
61. Fox, J. D., and Robyt, J. F. (1991) *Anal. Biochem.* **195**, 93–96
62. Berman, H. M., Westbrook, J., Feng, Z., Gilliland, G., Bhat, T. N., Weissig, H., Shindyalov, I. N., and Bourne, P. E. (2000) *Nucleic Acids Res.* **28**, 235–242
63. van der Veen, B. A., Leemhuis, H., Kralj, S., Uitdehaag, J. C., Dijkstra, B. W., and Dijkhuizen, L. (2001) *J. Biol. Chem.* **276**, 44557–44562
64. Svensson, B. (1994) *Plant Mol. Biol.* **25**, 141–157
65. Rodenburg, K. W., Vallée, F., Juge, N., Aghajari, N., Guo, X., Haser, R., and Svensson, B. (2000) *Eur. J. Biochem.* **267**, 1019–1029
66. Svensson, B., Bak-Jensen, K. S., Jensen, M. T., Sauer, J., Gottschalk, T. E., and Rodenburg, K. W. (1999) *J. Appl. Glycosci.* **46**, 49–63
67. Rappenecker, G., and Zugenmaier, P. (1981) *Carbohydr. Res.* **89**, 11–19
68. Imberty, A., Chanzy, H., Perez, S., Buleon, A., and Tran, V. (1988) *J. Mol. Biol.* **201**, 365–378
69. Wilkinson, A. J., Fersht, A. R., Blow, D. M., and Winther, G. (1983) *Biochemistry* **22**, 3581–3586
70. André, G., Jensen, M. T., Svensson, B., and Tran, V. (2003) in *Recent Advances in Enzymes in Grain Processing* (Courtin, C. M., Veraverbeke, W. S., and Delcour, J., eds) pp. 9–14, Katholieke Universiteit Leuven, Leuven
71. Stone, B. A., and Svensson, B. (2001) in *Glycoscience: Chemistry and Chemical Biology* (Fraser-Reid, B., Tatsuta, K., and Thiem, J., eds) pp. 1907–1990, Springer Verlag, Berlin/Heidelberg
72. Koivula, A., Kinnari, T., Harjunpää, V., Ruohonen, L., Teleman, A., Drakenberg, T., Rouvinen, J., Jones, T. A., and Teeri, T. T. (1998) *FEBS Lett.* **429**, 341–346
73. Varrot, A., Hastrup, S., Schülein, M., and Davies, G. J. (1999) *Biochem. J.* **337**, 297–304
74. Zou, J., Kleywegt, G. J., Ståhlberg, J., Driguez, H., Nerinckx, W., Claeysens, M., Koivula, A., Teeri, T. T., and Jones, T. A. (1999) *Struct. Fold. Des.* **7**, 1035–1045
75. Frandsen, T. P., Stoffer, B. B., Palcic, M. M., Hof, S., and Svensson, B. (1996) *J. Mol. Biol.* **263**, 79–89
76. Sierks, M. R., and Svensson, B. (2000) *Biochemistry* **39**, 8585–8592
77. Armand, S., Andrews, S. R., Charnock, S. J., and Gilbert, H. J. (2001) *Biochemistry* **40**, 7404–7409

**Tyrosine 105 and Threonine 212 at Outermost Substrate Binding Subsites –6 and +4 Control Substrate Specificity, Oligosaccharide Cleavage Patterns, and Multiple Binding Modes of Barley  $\alpha$ -Amylase 1**

Kristian Sass Bak-Jensen, Gwenaëlle André, Tine E. Gottschalk, Gabriel Paës, Vinh Tran and Birte Svensson

*J. Biol. Chem.* 2004, 279:10093-10102.

doi: 10.1074/jbc.M312825200 originally published online December 1, 2003

---

Access the most updated version of this article at doi: [10.1074/jbc.M312825200](https://doi.org/10.1074/jbc.M312825200)

Alerts:

- [When this article is cited](#)
- [When a correction for this article is posted](#)

[Click here](#) to choose from all of JBC's e-mail alerts

This article cites 68 references, 10 of which can be accessed free at <http://www.jbc.org/content/279/11/10093.full.html#ref-list-1>